Romanian Reports in Physics, Vol. 68, No. 2, P. 713–724, 2016

OPTICS

FOURIER-TRANSFORM INTERFERENCE LITHOGRAPHY

M. BULINSKI[1], G. MOAGĂR-POLADIAN[2*]

[1] Faculty of Physics, Bucharest University, 405 Atomiştilor St., Bucureşti – Măgurele, România
[2] National Institute for Research and Development in Microtechnology,
126A Erou Iancu Nicolae St., Bucureşti, România
* E-mail: gabriel.moagar@imt.ro

Received July 17, 2014

Abstract. Starting from the concept of interference lithography, developed several years ago, which is currently used in fabrication of 2D and 3D simple shapes periodical structures in so called holographic lithography, or laser lithography, we analyze in this paper the possibility of practical application of the concept for the realization of non-periodic patterns into a commercial photoresist.

Key words: interference lithography, non-periodic patterns, binary and grey lithography.

1. INTRODUCTION

Today, the realization of micro- and nanostructures by using low-cost and rapid methods has attracted a lot of attention and research, since the applications of such reduced scale structures are very important, aiding diverse disciplines from engineering to materials to medicine and biology, as well as security [1–2]. Fulfilling the cost and time requirements have proven to be the advantage of light based solutions, since light may realize many structures in parallel. While usual optical lithography techniques [3–4] have reached maturity and have proven ability to go to feature dimensions as low as 32 nm [5] the complexity and costs associated with such elaborated optical lithography techniques make them not affordable for many users interested to produce and apply nanostructures.

For the case of periodic structures, *interference lithography* (IL) [6–8] has proven a useful, low-cost and easy-to-implement technique for various applications. The main limitation of IL is that it can produce only periodic structures. One such development is that of [9] who have proven the possibility to realize non-periodic patterns by interference lithography, which is used by us to analyze its practical applicability and its limitations.

Recent scientific and technological developments require special lithography techniques for the manufacturing of complex “greyscale” structures: photonic band gap crystals; micro and nano electro-mechanical systems; diffractive and refractive

micro-optics (array of a-spherical lenses; etc.). Multi-level or greyscale lithography is relatively underutilized today, and the most important reason is the difficulty to obtain a real a greyscale exposure [10]. Limitation to a discrete number of grey levels as well as the size of the light beam (pixel size) – specific to beam scanning systems – represents a hurdle when generation of complex surface profiles of the photoresist have to be obtained. This limitation of traditional techniques is one of the strengths of the method presented in this article.

1.1. INTERFERENCE LITHOGRAPHY AND NON-PERIODICAL PATTERNS

The intensity distribution along the spatial axis x for an interference pattern produced by two interfering beams of wavelength λ and equal amplitudes that are symmetrically incident onto the substrate at an angle θ with respect to the normal (Fig. 1) is given by [11]:

$$I(x, y \mid \Lambda) = I_0(\Lambda) \cdot \left(1 + \cos\left(\frac{2\pi}{\Lambda} x + \varphi_0\right)\right), \tag{1}$$

where $I_0(\Lambda)$ is the maximum intensity of the fringes, the spatial period Λ is

$$\Lambda = \frac{\lambda}{2\sin(\theta)}, \tag{2}$$

and the intensity distribution along y axis is constant. The interference figure is invariant to vertical translation. The intensity is formed by a constant background to which a harmonic component of spatial frequency Λ is added.

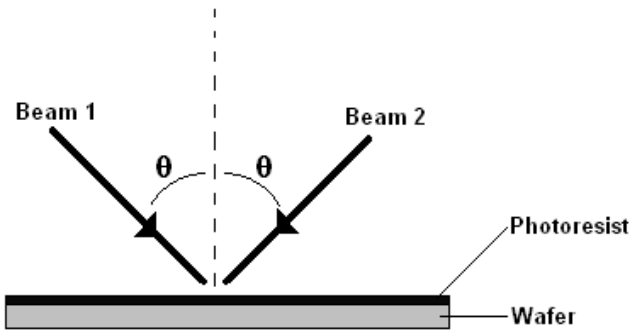

Fig. 1 – The geometry of the interfering beams.

For simplicity we discuss the 1D case, but the situation is similar in 2D or even 3D. Let consider a randomly chosen intensity pattern $J_{ideal}(x)$ (real and

positive by definition), of spatial length P, decomposed into a Fourier series [12] according to the expression:

$$J_{ideal}(x) = \sum_n H(k_n) \cdot \cos(k_n \cdot x + \varphi_n), \tag{3}$$

where n denotes the n^{th} component of the series (experimental values $n = 0, 1, ..., N$), $H(k_n)$ and φ_n represents the amplitude and phase of the n^{th} component and k_n is given by the expression:

$$k_n = \frac{2\pi}{P} n = \frac{2\pi}{\Lambda_n}, \tag{4}$$

representing a sum of cosines conveniently chosen.

The only difference between any spectral components of expression (3) and light intensity distribution that can be achieved by controlled interference is the constant background, present in (2). The interference pattern we plan to use for Fourier components of (3) may have only positive values for the light intensity, and this is why we can reconstruct the variations in the distribution of $J(x)$ only up to a constant factor. Using these "positive definite harmonic components", the Fourier reconstruction must have a constant positive component added to eq. (3)

$$J_{\exp}(x) = \sum_n J_0(\Lambda_n) + \sum_n J_0(\Lambda_n) \cdot \cos\left(\frac{2\pi}{\Lambda_n} x + \varphi_n\right), \tag{5}$$

This constant component may be regarded as the zero-frequency component that has a null initial phase. The first term in the right side of eq. (5) is a constant and its value is determined by the concrete distribution $J_{ideal}(x)$. The phase of the n component can be managed by the phase shift of one of the interfering beams.

We can obtain arbitrary non-periodic patterns as a superposition of harmonic components, similar to the synthesis of signals by using Fourier transforms. To synthesize the desired dose pattern (for lithographic purpose) up to a constant term, we use the superposition of periodic interference patterns each having corresponding intensity, spatial frequency and initial phase given by (5), see also [9]. These periodic intensity patterns, obtained by interference, accordingly with Fourier transform of the initial / desired dose pattern, are superposed onto the photoresist, one after each other, by taking advantage of the cumulative and non-linear response specific to this material. Because it is based on the Fourier transform of the desired pattern, we call this type of lithography as Fourier Transform Interference Lithography (**FTIL**).

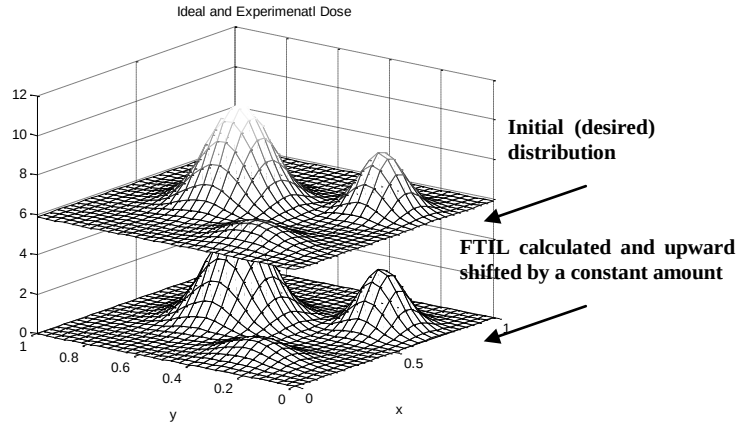

Fig. 2 – The background contribution of positive definite harmonic components.

The generation of the desired pattern into the photoresist is made as follows: 1) The desired pattern thickness distribution is converted to the required dose distribution taking into account the photoresist contrast curve. The dose distribution thus obtained represents the "ideal" dose distribution, *i.e.* the dose distribution that precisely describes the pattern. 2) A Fourier transform is made to the "ideal" dose distribution (for N components) for obtaining the illumination Fourier spectrum. 3) First M most energetically components are chosen (in descending energetically order) and used further in the dose distribution reconstruction. "Most energetically" must be understood as those components that bring quickly the resultant dose distribution close to the "ideal" one (*i.e.* within the accuracy limits agreed by the user). 4) The photoresist is illuminated with these M components (interference patterns) according to their incidence angle (given by the spatial frequency), intensity and initial phase, one component after the other. A supplementary constant exposure may be required to lead distribution into the photoresist response domain. 5) The photoresist is processed further according to the usual techniques.

In this paper we do not consider the simulation of the chemical development of the irradiated photoresist but only the aerial and latent images together with datasheet photoresist contrast curve.

One of the issues raised by the equation (5) is the vertically displacement of the initial distribution. To get an idea of the corresponding difference (ecart) let's calculate the resulting distribution by FTIL method, applied to an "ideal" sum of three 2D Gaussians, having maximum amplitudes of, respectively, "5", "3" and respectively "1" (Fig. 2).

Mentioning again that the value of this displacement is dependent on the distribution itself, we can see that for this basic case, the ecart is acceptable, being little larger than the maximum value of the initial distribution. This experimental

dose displacement can be compensated in the final photoresist thickness by the nonlinear response of the material, as will be shown below.

2. SIMULATION OF A FTIL PROCESS ON A COMMERCIAL PHOTORESIST

In order to simulate a FTIL process we consider the positive photoresist MICROPOSIT S1813 [13], having an experimental contrast curve and an idealized curve (used in simulations), presented in Fig. 3. y is the relative thickness of the photoresist, *i.e.* actual thickness t (after illumination) divided by the initial thickens t_0 (non-illuminated).

For a higher contrast photoresist, we may use the EPG 535 EverLight Chemical resist [13]. According to this photoresist datasheet the linear portion of the contrast curve is described by the equation: $y = 13.1395–5.8909 \cdot x$, x is the logarithm (base 10) of the incident dose (in mJ/cm^2).

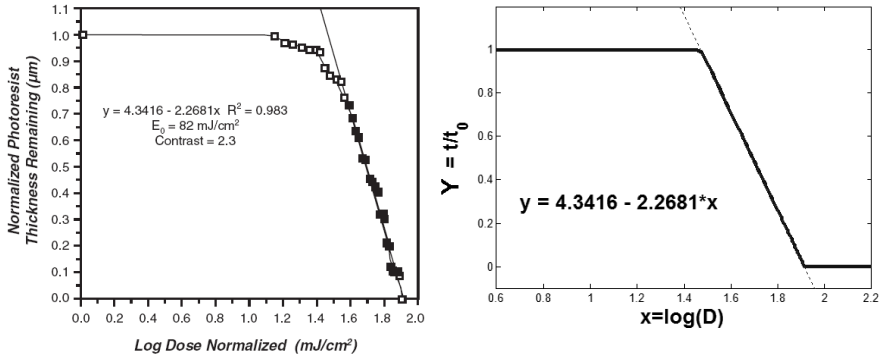

Fig. 3 – The photoresist contrast curve: a) the MICROPOSIT S1813 G2 Photoresist contrast curve [13]; b) idealized response used for simulation.

The photoresist contrast γ is defined as: $\gamma^{-1} = \lg(D_{100}) – \lg(D_{100})$, where D_0 is the light dose at which removal of the photoresist starts and D_{100} is the light dose that is necessary for the complete removal of the photoresist. D_{100} depends on the photoresist thickness.

For the S1813 photoresist, $\gamma = 2.3$ and $D_{100} = 82$ mJ/cm^2, while $D_0 = 30$ mJ/cm^2. The S1813 layer thickness is 1.2 microns. For the EPG 535 photoresist the parameters are $\gamma = 5.89$, $D_{100} = 170$ mJ/cm^2, while $D_0 = 115$ mJ/cm^2. The EPG 535 photoresist thickness is 1 micron. We consider two photoresists with different contrast value in order to demonstrate the influence of the contrast when reconstructing the pattern.

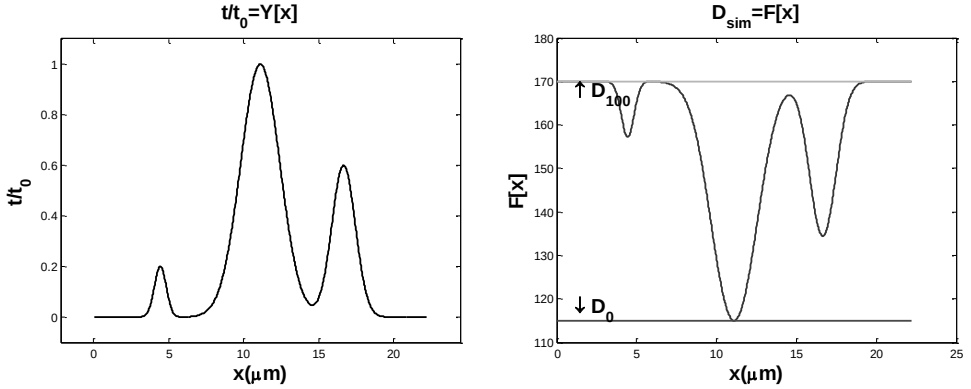

Fig. 4 – A grey level pattern and the exposure dose FTIL reconstruction, D_{sim}, for a positive EPG 535 photoresist: left – desired relative thickness (t_0 = total thickness of the photoresist); right – corresponding exposure dose (mJ/cm^2), with $F(x)$ = exposure dose.

First we consider an example of a 1D grey level pattern synthesis, Fig. 4, representing a sum of three Gaussians. After reconstructing the exposure dose, D_{sim}, we use the EPG 535 photoresist contrast curve to compute the variation of the photoresist thickness. For a number of only M = 20 Fourier components, the reconstruction error ($\mathrm{d}Y = \max(Y_{sim} - Y_{ideal})$) is d$Y \cong$ 4e–3; while for M = 100 the error decrease to d$Y \cong$ 4e–6, a very good reconstruction we may say.

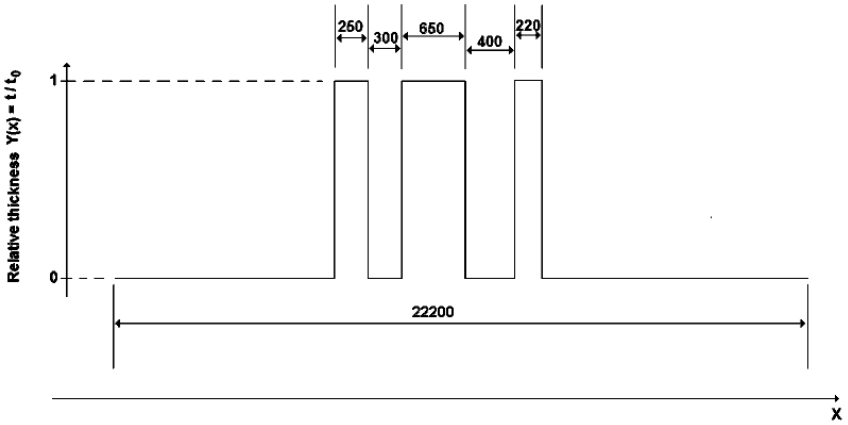

Fig. 5 – The desired photo-resist relative thickness distribution after development (in nanometers).

For testing a binary pattern synthesis, let's take a 1D pattern with the geometric distribution as that in Fig. 5.

After reconstructing the exposure dose D_{sim} (Fig. 6), using the corresponding photoresist contrast curve indicated into the figure, we compute the variation of the final photoresist thickness. The results showing the distribution of the relative

thickness Y of the photoresist is represented in Fig. 7 and shows how the initial pattern of Fig. 5 is reconstructed by using the FTIL method by using a number of M = 140 Fourier components. In Fig. 8 we present another reconstruction, less accurate, of the same structure but in this case with fewer Fourier components, M = = 80.

As is seen from the examples above, the reconstruction of the desired non-periodic pattern is obtained with enough accuracy using a number of 140 spatial frequency components. Moreover, the pattern is repeated over a distance d_0 of 22.2 microns. Figures 7 and 8 clearly show that a better reconstruction needs a higher number of components for obtaining more accurate photoresist margins and photoresist profile. On the other hand, the photoresist having a higher contrast gives better results as regards binary pattern reconstruction, as expected.

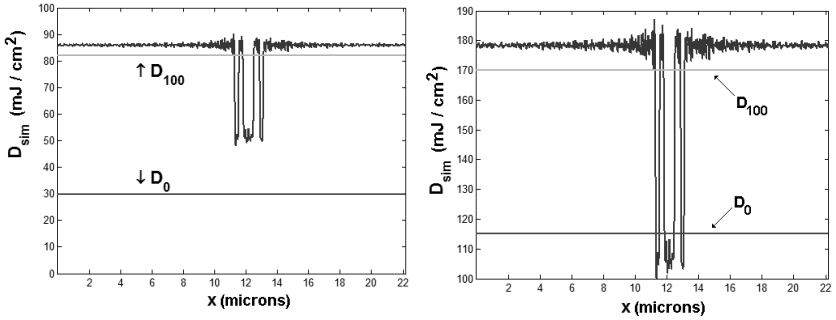

Fig. 6 – The exposure dose FTIL reconstruction for the pattern in Fig. 5 for a positive photoresist: a) the S1813 photoresist; b) the EPG 535 photoresist.

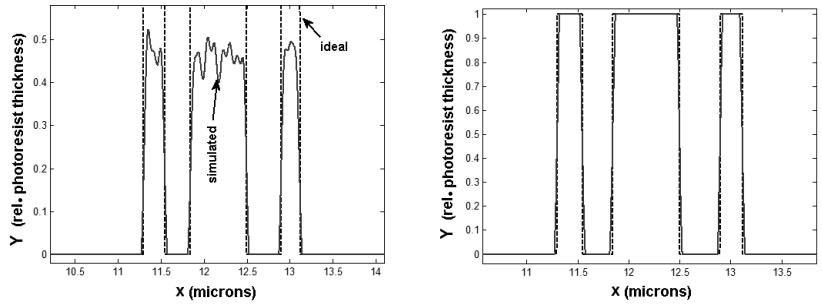

Fig. 7 – An augmented view of the reconstructed region from Fig. 5. The relative thickness of the photo-resist obtained by FTIL reconstruction (continuous line) *versus* ideal photo-resist relative thickness distribution Y_{ideal} (dashed line), when using a number of M = 140 components; a) refer to S1813 photoresist; b) refer to EPG 535.

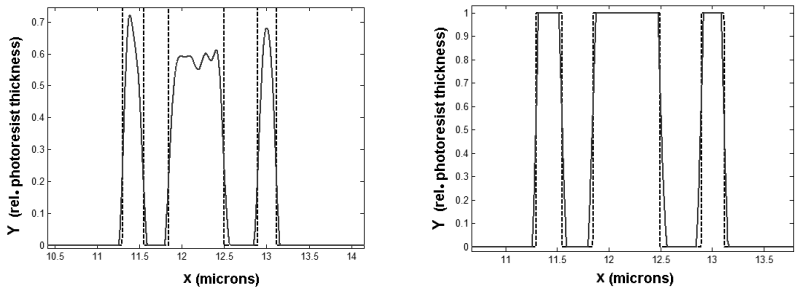

Fig. 8 – The same as in Fig. 7 but with reconstruction made by using fewer components (M = 80).

By comparing the width of the obtained pattern with that of the desired one we observe that the variation of the width at the top of the pattern does not exceed 10 % while at the bottom (at the substrate) is less than 5 %. These are acceptable values for width variation and prove the power of FTIL.

Another observation is that a lower contrast photoresist is thinned more than a higher contrast one during FTIL process.

One of the problems that might appear in such a lithographic technique is the ability to have a narrow pattern in the vicinity of a larger one. The simulations can prove the ability of FTIL to fairly overcome even a major limitation like that of two lines of largely different widths placed each in the vicinity of the other. This is an advantage compared to IL and other optical lithography methods such as near-field based ones. The reconstructed pattern quality may be improved by using a thinner photoresist layer, the value of D_{100} being thus decreased (γ increases). If the photoresist is thin enough, then the reconstructed pattern quality will be quite good.

We have to outline here that the multi-exposure technique in IL was used up to know (see for example [15–16]) but in all cases the patterns obtained were periodical. The respective structures were formed by different elementary objects (semi-sphere, ellipsoids, etc.) that were repeated onto the substrate at distances of a few radiation wavelengths. In our case, the structures obtained may have any pattern that is desired and that is non-periodic in its nature, while the pattern repetition length (for the case of reconstruction with summation of spatial frequencies harmonics) may reach few tens of microns independently on the size and shape of the elements contained by the non-periodic pattern. These are the main differences between FTIL and usual multi-exposure IL.

A very important advantage of FTIL is related to the fact that the interference pattern is invariant with respect to the vertical movement (*i.e.* along a direction perpendicular to the substrate) so that no vertical misalignment may appear. In this way, the problem of depth-of-focus (DOF) as encountered in mask-based photolithography is avoided. This opens up the ability to use very thick photoresists provided that enough light exposure is provided (D_{100} increases with

photoresist thickness). The advantages of FTIR method can include: does not use expensive masks; no critical optical alignment is necessary (except for the case when alignment of the non-periodic pattern with respect to previous realized structures is necessary); can be used for both binary and grey lithography; relatively few exposure steps can be used for acceptable errors; etc. Moreover, it allows the creation of surfaces with a complex 3D profile in thick photoresists.

3. CONSTRAINTS OF THE FTIL TECHNIQUE

As already mentioned, one of the limitations of the FTIL technique is represented by the background term in (5). This background term is equal to the displacement of the ideal distribution obtained by summation of corresponding interference figures. This term, expressed as exposure dose, should allow us to expand the experimental dose (Fig. 4) into the linear part of the contrast curve (Fig. 3). Otherwise the correct reconstruction of the desired shape is not possible.

The number $M_{\max}$ of available spatial frequencies is given by the relation:

$$M^{(h)}_{\max} = \frac{\sin(\theta_{\max})}{\sin(\theta_{\min})},\ M^{(c)}_{\max} = \frac{\theta_{\max} - \theta_{\min}}{\Delta\theta}, \tag{6}$$

where $\theta_{\max}$ and $\theta_{\min}$ are maximum, respectively minimum, angles of incidence allowed by the FTIL system and $\Delta\theta$ is the minimum variation of the incidence angle attainable by the FTIL system. $M_{\max}^{(h)}$ represents the maximum number of spatial frequencies for the case of using harmonic components (multiples) of a fundamental spatial frequency (as for Figs. 4–10). $M_{\max}^{(c)}$ represents the maximum number of spatial frequencies when using a "continuous" spectrum of spatial frequencies (between $\theta_{\min}$ and $\theta_{\max}$ in steps of $\Delta\theta$).

For the case $\theta_{\max} = 89^{o}$, $\theta_{\min} = 1^{o}$ and $\Delta\theta = 0.1^{o}$. $M_{\max}^{(h)} = 57$ and $M_{\max}^{(c)} = 880$. If the minimum angle of incidence can be lowered to 0.1^{o} and $\theta_{\max} = 89^{o}$, then $M_{\max}^{(h)} = 572$ and $M_{\max}^{(c)} = 889$. From these values it results that the angular resolution and minimum achievable angle of incidence are the critical parameters for any FTIL system.

Another parameter of interest, related to the angular resolution, is the beam divergence of the light source. Since today lasers and collimating optics have a divergence of less than 1 mrad, it results that the beam divergence may not affect practically the FTIL process. However, the minimum variation of the incidence angle cannot be made as small as we wish because then the beam divergence will put a limit to it.

The main limitation of the FTIL method is represented by the highest available spatial frequency component that can be used for reconstructing the desired pattern and by the number of frequency components used for reconstruction. This limits the accuracy of the final dose reconstruction by the

maximum number M_{max} of Fourier frequency components that can be achieved with a set of experimental parameters.

A larger repetition distance of the main pattern, P, can be obtained by increasing the smallest spatial frequency component used, and of course the total number of frequencies involved. Sometimes, a pattern like that in figure 5 have to be encountered only once (at one location) onto a 1 mm × 1 mm chip. As results from the previous paragraphs, the repetition length is of the order of tens of microns. This fact poses problems since the maximum number $M_{\max}$ of available spatial frequencies is limited. It results that it is not possible to create a non-periodic pattern that is able to cover a whole wafer or large parts of it.

At large angles of incidence, if we use beams whose diameters are small compared to the wafer size, then the overlap region of the interfering beams will increase as the angle of incidence is increased. Only the photoresist in the regions illuminated with all the needed spatial frequencies will be fully developed. This limitation may be overcome by using large area masks (cheap technologically) to delimit the interest region or by using beams whose diameters are of the same size as the wafer. Another possibility to delimitate the interest regions is to use of a uniform pre-illumination solely in the regions where the pattern must exist (at a dose lower than the D_{100} value), or laser ablation to the unwanted portions to be processed – less expensive and less complex than usual photolithography since it is made on areas of few tens of microns size and even larger than that. However, it must be taken into account that only the photoresist in the regions illuminated with all the needed spatial frequencies will be fully developed. The resist in the regions illuminated only at large angles of incidence will be thinned after development but will be not removed completely.

One other aspect to be considered is related to the distribution of the desired intensity pattern. In order to obtain an overall exposure dose, which correlated with the photoresist response curve, generates a pattern like that in Fig. 2 (*i.e.* rectangular edges), we need to use many high spatial frequencies Λ. The higher is the number of spatial frequencies (and hence the exposure needed) the higher is the constant background from the interference patterns. This has as a result the lowering of fringe contrast (visibility). The photoresist will be thinned substantially, also. Because of that, thicker photoresists are an option in such cases, especially due to the fact the interference pattern is invariant to the vertical translation. However, a thicker photoresist means a lower contrast γ and hence a less accurate reconstruction. A balance has to be made in these cases.

If only certain “continuous”/ grey 3D profiles of the photoresist surface are needed (as opposed to binary ones), then the thickness bias does not represent a problem anymore. This is the case of structures made for example for the static optical wavefront correction, for phase masks for advanced lithography or for embossing of different type of microstructures.

A strong requirement is that the intensity profile of the beams, when projected onto the wafer surface, be uniform. Today, such top-hat profiles are achievable with specially designed optics, so that this requirement may be fulfilled.

As mentioned previously, it is of utmost importance for binary profiles to have resists with high contrast value. The value of the photoresist contrast may represent, in some cases, a major limitation for the FTIL process application (especially in the visible region).

We must also mention that FTIL is a serial technique, namely the illumination of the photoresist with different Fourier frequency components is made in a serial manner, one after the other. Because of that, one may object that FTIL is a method taking too much time and thus is impractical. This is not necessarily the case, since the intensity of the light source can be increased enough so as to reduce the lithography time to a reasonable value. The only important parameter is the total dose that has to be obtained onto the photoresist. Depending on the light intensity used, the FTIL process may take between few seconds up to few tens of seconds.

Finally, all the aspects considered in the paper are applicable to liquid as well as to solid (such as the As_2S_3:Ag system) photoresists.

4. CONCLUSIONS

In this paper we have studied and analyzed the method of interference lithography used for obtaining non-periodic patterns, FTIL. Through numerical simulations we have shown that it is possible to obtain complex, arbitrary non-periodic patterns, binary or grey, into a commercial photoresist. We discussed the main intrinsic limitations of FTIL and some methods to mitigate them. Fourier-transform interference lithography can be a possible alternative to classical projection lithography, without expensive masks, using the photoresist nonlinearities under controlled direct dose exposure, with practical applications in binary or grey lithography.

Acknowledgements. This work was performed under the project IDEI contract no. 62 / 2011 financed by UEFISCDI.

REFERENCES

1. J. Xavier, M. Boguslawski, P. Rose, J. Joseph, C. Denz, Adv. Mater. **22**, 356–360 (2010).
2. P. Srinivasan, *Design and fabrication of space variant micro optical elements*, PhD Thesis, University of Central Florida, Orlando, Florida, 2009.
3. K. Bubke, E. Cotte, J. H. Peters, R. de Kruif, M. Duşa, J. Fochler, B. Connolly, J. Micro/Nanolith. MEMS MOEMS, Vol. 8 (24th European Mask and Lithography Conference), Dresden, 2009.

4. G. Bjork, L. L. S. Soto, J. Soderholm, Phys. Rev. A **64**, p. 013811 (2001).
5. M. Freebody, Photonics Spectra, May 2011.
6. S. Kuiper, H. Van Wolferen, C. van Rijn, W. Nijdam, G. Krijnen, M. Elwenspoek, J. Micromech. Microeng. **11**, p. 33–37 (2001).
7. X. Yang, B. Zeng, C. Wang, X. Luo, Optics Express **17**, no. 24, p. 21560–21565 (2009).
8. J. Xavier, S. Vyas, P. Senthilkumaran, J. Joseph, International Journal of Optics, Article ID 863875 (2012).
9. S. Pau, G. P. Watson, O. Nalamasu, J. Mod. Optics **48**, 1211 (2001).
10. McKenna, C., Walsh, K., Crain, M., Lake, J., Micro/Nano Symposium (UGIM), 2010, 18th Biennial University / Government / Industry.
11. M. Born, E. Wolf, *Principles of Optics*, Cambride University Press, 7th edition, 1999.
12. E. O. Brigham, *Fast Fourier Transform and its Applications*, Prentice Hall, 1988.
13. Rohm and Haas Electronic Materials © 2006 – MicropositTM SI800TM G2 Series Photoresists for Microlithography Applications.
14. EPG 535 datasheet from EverLight Chemical, http://www.everlightchemical-ecbu.com/EN/product_detail_1.asp?detail_seq=18 (June 2012).
15. C. J. M. van Rijn, J. Microlith., Microfab., Microsyst. **5**, *1*, 011012 (2006).
16. D. Xia, Z. Ku, S. C. Lee , S. R. J. Brueck, Adv. Mater. **23**, 147–179 (2011).